Urban Carbon Emission Control and Economic Security Evaluation Based on BP Artificial Neural Network

DOI: 10.23977/infse.2025.060220

ISSN 2523-6407 Vol. 6 Num. 2

Wanjun Xie^{1,a}, Junhui Zhou^{2,b,*}

¹College of Architectural Engineering, Science and Technology College of Hubei University of Arts and Science, Xiangyang, 441025, Hubei, China

²Haibo Heavy Engineering Science and Technology Company Limited , Wuhan, 430000, Hubei, China

> ^axww20230701@163.com, ^bjun20170419@163.com *Corresponding author

Keywords: Neural Network; Urban Carbon Emissions; Carbon Emission Control; Economic Security

Abstract: Global warming is a critical environmental challenge threatening human survival and China's sustainable economic development. The scientific consensus attributes it partly to rising carbon emissions from human activities, a problem exacerbated by its own consequences. The Kyoto Protocol established a global emissions reduction framework, and many industrialized nations have taken action. As a major emitter, China faces growing international pressure to cut emissions, making urban carbon control a key research focus—though it is more accurately a topic in environmental and policy studies, not the medical community. This paper conducts experiments on urban carbon emissions and economic security using a BP artificial neural network. Results show that after optimization, the pressure system's carbon emission economic security index steadily declined from 0.667 in 2013 to 0.204 in 2024, offering a clear direction for improving urban carbon emission management and economic security.

1. Introduction

Global heating is a major concern for the global industry, primarily driven by rising carbon dioxide levels, as confirmed by the UN IPCC. As the world's largest energy consumer, China faces significant pressure to reduce its energy output. Meanwhile, China's rapid urbanization—soaring from 18.57% in 1978 to 58.52% in 2017—acts as a powerful engine for social and cultural advancement. Urbanization is a key indicator of national development, and with nearly half the world's population now living in cities and China accounting for about one-fifth of humanity, its urbanization plays a critical global role. According to U.S. researchers, urbanization follows an S-shaped curve: below 30% it progresses slowly; between 30% and 70% it accelerates; and beyond 70% it stabilizes. China is currently in the acceleration phase, and a Nobel laureate in economics has emphasized that China's urbanization, together with U.S. high technology, will be pivotal to humanity's 21st-century future.

With rapid urbanization, cities—though the most prosperous and resource-rich areas—face growing challenges. A survey of Chinese cities' "happiness index" shows declining life satisfaction

among urban residents. Issues like traffic congestion, inadequate education and healthcare, and environmental pollution have emerged, placing immense pressure on resources and sustainability. Therefore, urbanization must shift from extensive expansion and increasing city numbers to intensive, quality-driven development that enhances urban living standards.

This paper investigates urban carbon emissions and economic security using a bp artificial neural network. Results show that, since 2013, all prefecture-level cities in shaanxi have maintained at least a critical safety level—eliminating the unsafe states observed before optimization. From 2014 to 2017, Tongchuan was in critical safety (4-year average: 0.529), while Baoji was safe (average: 0.619). From 2018 to 2021, all cities were in critical safety (averages: 0.581 for Xi'an, 0.564 for Baoji, 0.586 for Tongchuan), with little change from 2022 to 2024. Post-optimization, the response system's economic security index peaked at 0.860 in 2024, while the pressure index steadily declined from 2019 to 2023. These findings demonstrate that the BP neural network approach significantly enhances urban carbon emission management and economic security, offering valuable guidance for sustainable urban development.

2. Related Work

As global warming intensifies, urban carbon emission control and economic security have become central to international environmental governance and sustainable development research. Existing studies primarily examine urban carbon drivers through energy consumption structure [1–2], industrial layout, population growth, and transportation, using carbon source analysis and carbon intensity accounting [3–4] to assess city-level emission performance. Chinese scholars have also developed decoupling models between emissions and economic growth and simulated low-carbon city pathways, employing tools like system dynamics, input-output analysis, and ecological footprint methods for quantitative analysis of the emission–economy relationship [5–6]. However, under heterogeneous multi-source data and complex dynamic feedback, traditional models lack sufficient prediction accuracy and nonlinear fitting capability, struggling to handle the high-dimensional and dynamic nature of urban carbon management and economic security evaluation. Thus, integrating artificial intelligence to enhance analytical and predictive intelligence is urgently needed.

In recent years, BP neural networks have been widely applied in environmental modeling and economic risk assessment due to their strong nonlinear mapping, self-learning, and fault tolerance capabilities. Studies have used BP networks [7–8] to predict urban carbon emissions by incorporating inputs like energy structure, industrial activity intensity, and policy regulation, significantly improving fitting accuracy and dynamic response to emission trends [9–10]. BP networks have also been employed to build urban economic security indices, aiding analysis of the coupling between environmental pressure and economic carrying capacity. However, most existing research fails to fully integrate "carbon emission control" [11–12] and "economic security assessment," and their models remain static with limited generalization. Thus, applying BP neural networks to integrated, multi-period modeling of urban carbon emissions and economic security holds significant theoretical and practical value for enhancing evidence-based green urban development strategies.

3. Overview of Neural Networks for Urban Carbon Emissions and Economic Security

3.1 Overview of Artificial Neural Networks

The BP neural network, inspired by biological neurons, is a feedforward multilayer architecture that processes information through forward propagation and learns through backward error propagation. During training, the network iteratively adjusts its weights and thresholds based on output errors, enabling it to effectively handle nonlinear problems. This structure ensures strong

adaptability and robustness in practical applications [13].

Bp network is mainly used for feature approximation, pattern recognition, data compression and so on. In traditional fields, 80-90% of network models are computed using bp networks or variants of bp networks, mostly using computer languages.

Artificial neural networks are theoretical statistical models inspired by the structure and function of the human brain. Composed of numerous interconnected neurons (processing units), they form a large-scale nonlinear adaptive system capable of handling uncertain information. When presented with input patterns similar to training samples, the system can infer results within an acceptable error margin.

Among artificial neural networks, the BP neural network is the most well-known. Its core is the error backpropagation algorithm—the most widely used learning method in neural networks—which adjusts weights and thresholds layer by layer from the output to the input layer, following the gradient of error reduction. This endows BP networks with strong adaptability and nonlinear mapping capability in practice [14].

BP neural network is an influential neural model proposed in 1986, and its most basic component is neurons. The artificial neuron model is shown in Figure 1:

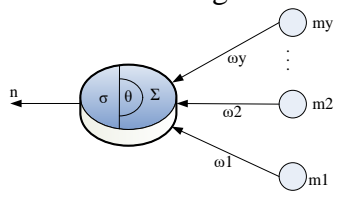


Figure 1: Artificial neuron model.

m represents the input information, ω represents the weight of the input information, Σ represents the weighted summation of the input information and weights, θ represents the threshold of the neuron, and σ represents the excitation function of the neuron [15]. The relationship between the output and input of a neuron is expressed by the Formulas:

$$p_i = [p_1, p_2...p_r]^T, i = 1, 2...r$$
 (1)

$$w_{j} = [w_{1}, w_{2}...w_{r}], j = 1,2...r$$
 (2)

The output Formulas of the neuron model is expressed as:

$$net_i = \sum_{j=1}^{r} w_{ij} m_j + \theta$$
 (3)

$$f_i = (net_i) \tag{4}$$

 f_i is the neuron's output, the feature f is the activity feature or a transfer feature, and net is the net effect of activation. The weighted sum of the inputs to the neuron is:

$$u = \sum_{i=1}^{y} m_i w_i + b = \sum_{i=0}^{y} m_i w_i$$
 (5)

The weights and thresholds of neurons are variable, representing different connection strengths and activation states. The product of each input value and its corresponding weight value plus the weighted sum u of the threshold value represents the total input of the neuron, and the output of the neuron is expressed as:

$$n = f(u) \tag{6}$$

$$n = f\left(\sum_{i=1}^{y} m_i w_i + b\right) \tag{7}$$

$$n = f\left(\sum_{i=0}^{y} m_i w_i\right) \tag{8}$$

Neuron mathematical models primarily consist of weighted summation and activation (transfer) functions. The key difference among models lies in their choice of activation function, which determines the neuron's information processing characteristics. Different activation functions are selected based on the problem at hand, and commonly used ones fall into four categories:

Hard clipping functions are usually divided into two forms: step functions and sign functions. The step function is defined as:

$$n = f(u) = \begin{cases} 1, u \ge 0 \\ 0, u < 0 \end{cases}$$
 (9)

The symbolic function is defined as:

$$n = f(u) = \begin{cases} 1, u > 0 \\ 0, u = 0 \\ -1, u < 0 \end{cases}$$
 (10)

Linear functions are usually divided into two forms: general linear functions and piecewise saturated linear functions. k is the slope and $\pm r$ is the range of the output. A general linear function is defined as:

$$n = f(u) = ku \tag{11}$$

The segmented saturation linear function is defined as:

$$n = f(u) = \begin{cases} r, u \ge r \\ ku, |u| < r \\ -r, u \le -r \end{cases}$$
 (12)

Nonlinear activation functions are mainly of two types: the sigmoid (S-shaped) function and the hyperbolic tangent (bipolar S-shaped) function. The sigmoid maps the real number line to the interval (0, 1), while the hyperbolic tangent maps it to (-1, 1). Both functions and their derivatives are continuous and analytically simple. The sigmoid function is defined as:

$$n = f(u) = \frac{1}{1 + e^{-u}}$$
 (13)

The hyperbolic tangent function is defined as:

$$n = f(u) = \frac{e^{u} - e^{-u}}{e^{u} + e^{-u}}$$
 (14)

The probability function is used to indicate that inputs and outputs in respect of each another of a neuron is uncertain, while the random function is used to describe the probability that its output state is 1 or 0. Give the probability that a neuron's output is 1 (T is the temperature parameter):

$$P(1) = \frac{1}{1 + e^{-T}}$$
 (15)

The learning rule of BP neural network is called tutored learning rule, which is an error correction algorithm. The tutored learning structure is shown in Figure 2:

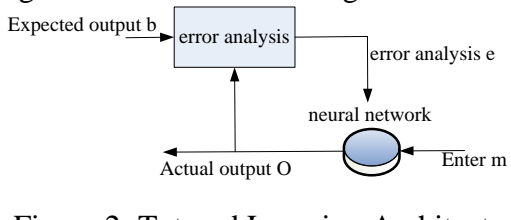


Figure 2: Tutored Learning Architecture.

During learning and training, the network is given an expected output, and a rule compares the

actual and desired outputs. If a discrepancy exists, the weights of each layer are adjusted—based on the direction, magnitude of the error, and a specific algorithm—to iteratively bring the actual output closer to the expected value. The unsupervised learning architecture of the neural network is shown in Figure 3:

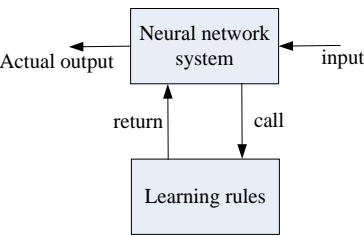


Figure 3: Unsupervised learning architecture.

In unsupervised learning, the neural network receives only input samples without corresponding correct outputs (teacher signals). It adjusts its weights based on the inputs, its internal structure, and predefined learning rules, with the learning criterion implicitly embedded in its own organization.

Compared with grey relational analysis, scoring, grey cluster analysis, and fuzzy mathematics, the BP artificial neural network offers distinct advantages in multi-index evaluation: massive parallel processing capability—transforming simple systems into ones capable of handling complex problems—robustness through distributed weight-based memory, and high adaptability, self-organization, accuracy, cost-effectiveness, and ease of use, as it autonomously adjusts weights to evolving data.

A neural network's computational performance depends on its activation functions and connection weights. The weights are critical parameters that determine whether the network meets design requirements and can only be determined through training. A typical neural network training process is as follows: The mathematical expression of Hebb's learning rule is:

$$w_{ij}(k+1) = w_{ij}(k) + \mu \cdot n_i(k) \cdot n_j(k)$$
 (16)

The basic learning rule of BP neural network is proposed based on the error learning correction method, and its weight correction Formula is:

$$(k+1) = w_{ij}(k) + \mu \left(d_j - n_i(k) \right) . m_i(k)$$
 (17)

The learning of neural network mainly includes three stages: forward propagation, error back propagation and weight update. The forward propagation stage expression is:

$$I_{j}^{g} = \sum_{i=1} \omega_{ij}^{g-1} O_{i}^{g-1} - \theta_{j}^{g}$$
 (18)

$$O_j^g = f\left(I_j^g\right) \tag{19}$$

In the error back propagation stage, the error function is the sum of the squares of the errors of the output neurons in each layer as follows:

$$e = \frac{1}{2} \sum_{j} (n_{j} - 0_{j}^{x})^{2}$$
 (20)

The BP neural network method is based on the orientation of the error in the direction of the positive scale. Each input to the network corresponds to an actual output. During training, the network has to adjust connection heights and thresholds based on the deviation between expected and actual outputs.

3.2 Overview of Carbon Emissions and Economic Security

Since the 1970s, severe environmental issues including droughts and climate anomalies have emerged worldwide, adversely affecting economic development and human welfare. Accelerated global expansion has driven extensive consumption of fossil fuels, rapidly increasing heat accumulation in the Earth system. According to the Fourth IPCC Assessment Report, global average temperatures were projected to rise by 2-4.2 °C by 2017. This warming triggers polar ice melt, permafrost thaw, sea-level rise, and disrupts atmospheric circulation patterns, ultimately altering global precipitation distribution.

As climate warming worsens, energy conservation and carbon reduction have become global priorities. The mainstream view holds that fossil fuel consumption is the primary driver of the rapid rise in atmospheric greenhouse gas concentrations. Reducing emissions inevitably requires cutting energy use, yet economic development depends heavily on energy consumption—creating a tension between emission reduction goals and the secure growth of the national economy.

Energy underpins human survival and socio-economic development, yet major sources like coal, oil, and natural gas are non-renewable or slowly renewable. Accelerated global industrialization has sharply increased energy demand, straining environmental resources. Thus, the key challenge is ensuring economic growth while achieving energy conservation, efficient use, and reduced pollution emissions.

The environmental system is the material basis for economic development; its collapse would destroy human habitats, undermine basic living needs, disrupt social order, and make economic development impossible. Their interdependent relationship in coordinated development is shown in Figure 4:

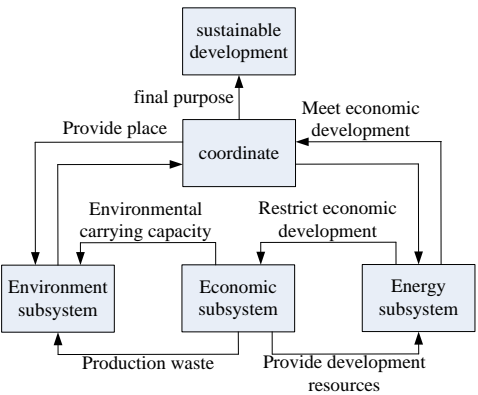


Figure 4: Coordinated development interaction.

Rapid economic development increases energy demand and environmental pressure, yet it also drives scientific and technological progress, enabling new energy development, energy-saving and emission-reduction technologies, and providing technical and financial support for ecological restoration.

A low-cost model embodies a low-carbon industrial approach—marked by low emissions, low pollution, and reduced dependence on high-carbon energy—by enhancing energy efficiency, lowering carbon intensity, and replacing fossil fuels with clean energy. It entails industrial restructuring: shrinking energy-intensive sectors and expanding technology-intensive ones, such as strategic emerging industries replacing outdated manufacturing. Internally, firms can switch to low-carbon energy (e.g., natural gas over coal) based on production needs. Beyond structural change, low-carbon development also requires raising public environmental awareness to promote energy-saving and sustainable consumption. As the world's largest emitter, China faces strong international pressure to cut emissions, yet its ongoing development demands high energy use—making a low-carbon

economic path the only viable option.

As awareness of the low-carbon economy grows, terms like "low-carbon campus," "society," "transportation," and "city" have popularized low carbon as a social norm and built public consensus. Governments advance this through policies—such as embedding low-carbon goals in national planning (administrative measures) and launching carbon markets (economic incentives). Individuals must also adopt low-carbon lifestyles by moving away from high-energy consumption, conserving resources, boosting efficiency, and avoiding waste and excess.

As global attention to urbanization's impact on carbon emissions grows, scholars increasingly study their relationship, focusing on urban–emission linkages, theoretical mechanisms linking cities (and firms) to carbon output, and regional differences in how urbanization affects emissions.

Although urbanization is often viewed as a facet of economic modernization, it is also a demographic process that increases urban density and alters residents' lifestyles—thereby influencing production patterns, energy use (especially in China), and urban pollution behaviors. However, no single theory fully or clearly explains urbanization's current impact on urban energy consumption and carbon emissions. The theoretical framework for urban environmental transformation is shown in Figure 5:

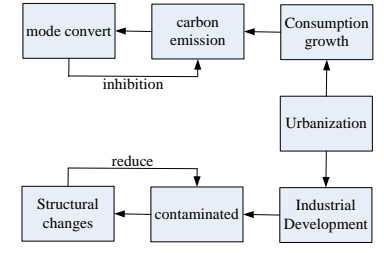


Figure 5: Theoretical logical framework of urban environmental transformation.

In highly urbanized developed cities, environmental pollution tends to decline due to stricter environmental controls, technological advances, and industrial restructuring. However, at advanced urbanization stages, consumption-related environmental issues may arise, as affluent residents often adopt more resource-intensive lifestyles than those in less-urbanized cities.

4. Urban Carbon Emissions and Economic Security before and after Improvement

4.1 Status Quo of Carbon Emission Economic Security

Process evaluation research is the most effective approach for dynamic change analysis, and carbon emission economic safety assessment employs this method. This section uses data analysis, selecting carbon emission economic safety data from 11 cities in Shaanxi Province over the 2013–2024 period for dynamic evaluation. The resulting comprehensive economic-safety values are shown in Figure 6:



Figure 6: 2013-2024 Comprehensive Value of Carbon Emission Economic Security.

As shown in Figure 6, the pressure system's carbon emission economic security index fluctuated downward from 0.777 in 2013 to 0.664 in 2024, indicating a slight increase in driving pressure. The response system's index rose modestly, ranging from a low of 0.164 in 2015 to a high of 0.251 in 2024, suggesting that mitigation measures have had some—though unstable—effect. The overall carbon emission economic safety values for 2013–2024 are presented in Figure 7:

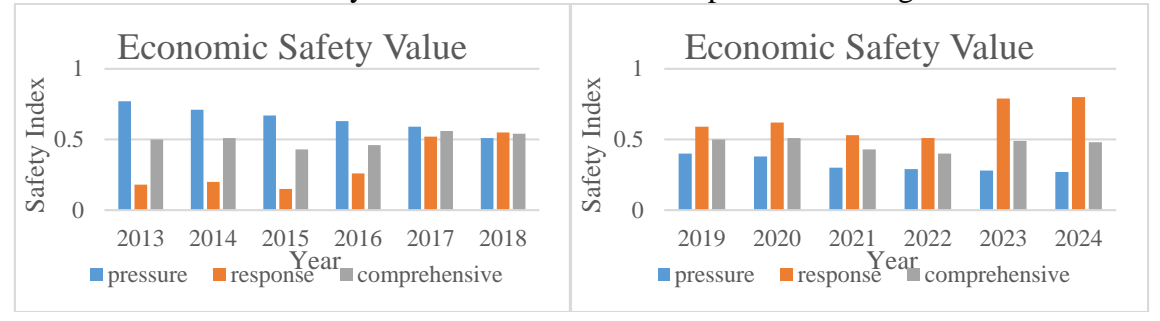


Figure 7: Economic safety value of carbon emissions from 2013 to 2024.

Figure 7 shows that the comprehensive index reflects the interplay between the pressure and response safety indices. Before 2018, the pressure index exceeded the response index, and carbon emission economic security improved as pressure declined. After 2018, the response index surpassed the pressure index, and security rose with stronger response measures. Further analysis reveals that accelerating urbanization in Shaanxi—marked by a steadily rising urbanization rate and rural-to-urban migration—has intensified population pressure in cities, driving significant carbon emission increases. The comprehensive carbon emission economic security index for Shaanxi's prefecture-level cities from 2013 to 2024 is shown in Figure 8:

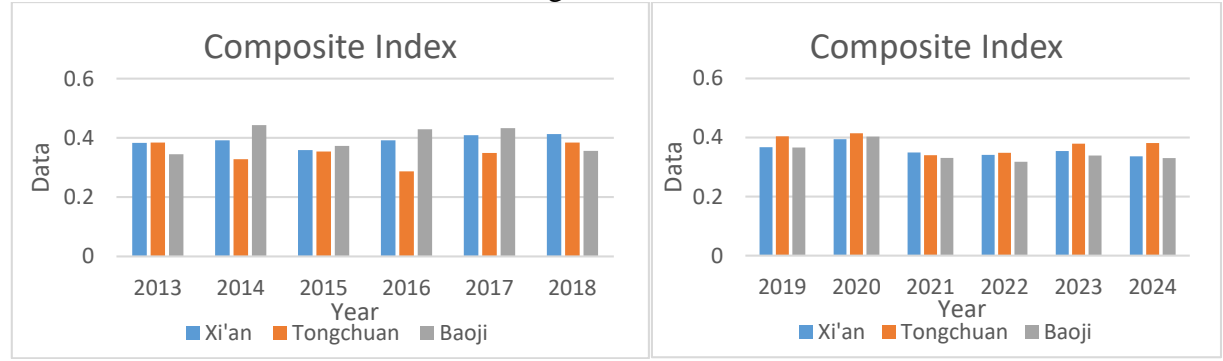


Figure 8: The comprehensive index of carbon emission economic security in Shaanxi prefectures and cities from 2013 to 2024.

As shown in Figure 8, Baoji was unsafe in 2013 (0.345). From 2014 to 2017, Tongchuan became unsafe, with a 4-year average of 0.329. Between 2018 and 2021, safety levels declined further, with Xi'an, Baoji, and Tongchuan all unsafe (averages: 0.381, 0.364, and 0.386, respectively). From 2022 to 2024, conditions changed little: Tongchuan improved to critical safety, while Xi'an and Baoji remained unsafe.

4.2 Economic Security of Carbon Emissions after Improvement of Artificial Neural Network

To address the carbon emission economic security issues identified earlier, this section introduces a BP artificial neural network to optimize carbon emissions. To verify the method's effectiveness, the same data analysis approach as in the previous section is applied. The improved comprehensive economic-safety values for 2013–2024 are presented in Table 1:

Table 1: The comprehensive economic and security value of carbon emissions from 2013 to 2024 after improvement.

Year	Pressure	Response	Comprehensive
2013	0.667	0.263	0.596
2014	0.625	0.300	0.604
2015	0.592	0.262	0.554
2016	0.579	0.384	0.602
2017	0.514	0.650	0.685
2018	0.442	0.673	0.656
2019	0.331	0.687	0.601
2020	0.299	0.755	0.614
2021	0.259	0.636	0.538
2022	0.220	0.616	0.508
2023	0.227	0.839	0.611
2024	0.204	0.860	0.611

As shown in Table 1, after BP neural network optimization, the pressure system's carbon emission economic security index steadily declined from 0.667 in 2013 to 0.204 in 2024. The improved response system's index reached a low of 0.262 in 2015 and a high of 0.860 in 2024—up from 0.164 and 0.251 pre-optimization, respectively—showing increases in both minimum and maximum safety levels, with the maximum rising by 0.609. The optimized carbon emission safety values for 2013—2024 are presented in Table 2:

Table 2: The improved economic safety value of carbon emissions from 2013 to 2024.

Year	pressure	response	comprehensive
2013	0.57	0.38	0.65
2014	0.51	0.40	0.66
2015	0.47	0.35	0.58
2016	0.43	0.46	0.61
2017	0.39	0.72	0.71
2018	0.31	0.75	0.69
2019	0.20	0.79	0.65
2020	0.18	0.82	0.66
2021	0.10	0.73	0.58
2022	0.09	0.71	0.55
2023	0.08	0.95	0.64
2024	0.07	0.99	0.63

As shown in Table 2, after BP neural network optimization, the pressure index in the carbon emission economic safety value dropped from 0.57 to 0.07—declining by 0.2 annually, compared to the pre-improvement drop from 0.77 to 0.27. The improved response index ranges from 0.35 to 0.99, up by 0.2 and 0.19 respectively from the pre-improvement range of 0.15 to 0.8. The comprehensive index also increased by 0.15 post-optimization. The improved 2013–2024 carbon emission economic security comprehensive index for Shaanxi's prefecture-level cities is shown in Table 3.

As shown in Table 3, after BP neural network optimization, all prefecture-level cities in Shaanxi were at least in a critical safety state from 2013 onward—eliminating the unsafe conditions seen before improvement. From 2014 to 2017, Tongchuan was in critical safety (4-year average: 0.529), while Baoji was safe (average: 0.619). From 2018 to 2021, all cities were in critical safety, with averages of 0.581 (Xi'an), 0.564 (Baoji), and 0.586 (Tongchuan). From 2022 to 2024, the situation

remained stable, with all cities staying in critical safety—occasionally reaching safe levels—showing consistent improvement over the pre-optimization period.

Table 3: The improved comprehensive index of carbon emission economic security in Shaanxi prefectures and cities from 2013 to 2024.

Year/region	Xi'an	Tongchuan	Baoji
2013	0.583	0.584	0.545
2014	0.592	0.528	0.643
2015	0.559	0.554	0.573
2016	0.592	0.487	0.629
2017	0.609	0.549	0.633
2018	0.613	0.584	0.556
2019	0.567	0.604	0.566
2020	0.594	0.614	0.603
2021	0.549	0.540	0.531
2022	0.541	0.548	0.518
2023	0.554	0.579	0.539
2024	0.536	0.581	0.530

5. Conclusion

As global environmental degradation worsens, climate change driven by greenhouse gas emissions has become a critical global concern. Rising emissions have increased temperatures, triggering severe environmental issues—such as sea-level rise, water imbalances, and ecosystem damage—that threaten human livelihoods and health. Effectively curbing carbon emissions is thus urgent. As the world's largest emitter, China faces intense international pressure to cut emissions. Urbanization, a key driver of China's future growth, significantly influences carbon emissions through economic agglomeration and urban energy consumption patterns. Therefore, studying the specific controls and regional differences in China's urban carbon emissions is crucial for promoting sustainable urbanization and achieving energy conservation and emission reduction.

References

- [1] Amen M A. The assessment of cities physical complexity through urban energy consumption[J]. Civil Engineering and Architecture, 2021, 9(7): 2517-2527.
- [2] Huang X, Zhu R, Wu X, Ge P. Assessing the role and driving mechanisms of the green financial reform on urban energy consumption and pollution emissions: a policy evaluation from the generalized synthetic control method[J]. Environmental Science and Pollution Research, 2023, 30(56): 119095-119116.
- [3] Wiedmann T, Chen G, Owen A, Lenzen M, Doust M, Barrett J, et al. Three-scope carbon emission inventories of global cities[J]. Journal of Industrial Ecology, 2021, 25(3): 735-750.
- [4] Miller G J, Novan K, Jenn A. Hourly accounting of carbon emissions from electricity consumption[J]. Environmental Research Letters, 2022, 17(4): 044073.
- [5] Shan Y, Fang S, Cai B. Chinese cities exhibit varying degrees of decoupling of economic growth and CO2 emissions between 2005 and 2015[J]. One Earth, 2021, 4(1): 124-134.
- [6] Zhong R, He Q, Qi Y. Digital economy, agricultural technological progress, and agricultural carbon intensity: Evidence from China[J]. International Journal of Environmental Research and Public Health, 2022, 19(11): 6488.
- [7] Zhang S, Huo Z, Zhai C. Building carbon emission scenario prediction using STIRPAT and GA-BP neural network model[J]. Sustainability, 2022, 14(15): 9369.
- [8] Feng W, Chen T, Li L. Application of Neural Networks on Carbon Emission Prediction: A Systematic Review and Comparison[J]. Energies, 2024, 17(7): 1628.
- [9] Wu S, Zeng X, Li C, Cang H, Tan Q, Xu D, et al. CO2 emission forecasting based on nonlinear grey Bernoulli and BP neural network combined model[J]. Soft Computing, 2023, 27(21): 15509-15521.

- [10] Li Y, Huang S, Miao L. Simulation analysis of carbon peak path in China from a multi-scenario perspective: evidence from random forest and back propagation neural network models[J]. Environmental Science and Pollution Research, 2023, 30(16): 46711-46726.
- [11] Sun W, Ren C. Short-term prediction of carbon emissions based on the EEMD-PSOBP model[J]. Environmental Science and Pollution Research, 2021, 28(40): 56580-56594.
- [12] Feng W, Chen T, Li L, Zhang L, Deng B, Liu W, et al. Application of Neural Networks on Carbon Emission Prediction: A Systematic Review and Comparison[J]. Energies, 2024, 17(7): 1628.
- [13] Luo J, Zhuo W, Xu B. A deep neural network-based assistive decision method for financial risk prediction in carbon trading market[J]. Journal of Circuits, Systems and Computers, 2024, 33(08): 2450153.
- [14] Tang J, Gong R, Wang H, Liu Y. Scenario analysis of transportation carbon emissions in China based on machine learning and deep neural network models[J]. Environmental Research Letters, 2023, 18(6): 064018.
- [15] Meng F, Dou R. Prophet-LSTM-BP ensemble carbon trading price prediction model[J]. Computational Economics, 2024, 63(5): 1805-1825.